



## RESEARCH ARTICLE

# Biomechanical Evaluation of Transforaminal Lumbar Interbody Fusion with Coflex-F and Pedicle Screw Fixation: Finite Element Analysis of Static and Vibration Conditions

Jia Zhu, PhD<sup>1,2,3</sup> , Hangkai Shen, PhD<sup>2,3</sup> , Yangyang Cui, PhD<sup>1,2,3</sup>, Guy R. Fogel, MD<sup>4</sup>, Zhenhua Liao, PhD<sup>3</sup>, Weiqiang Liu, PhD<sup>1,2,3</sup>

<sup>1</sup>Tsinghua Shenzhen International Graduate School, Tsinghua University and <sup>3</sup>Biomechanics and Biotechnology Lab, Research Institute of Tsinghua University in Shenzhen, Shenzhen and <sup>2</sup>Department of Mechanical Engineering, Tsinghua University, Beijing, China and <sup>4</sup>Spine Pain Begone Clinic, San Antonio, TX, USA

**Objective:** To investigate the biomechanics of transforaminal lumbar interbody fusion (TLIF) with interspinous process device (IPD) or pedicle screw fixation under both static and vibration conditions by the finite element (FE) method.

**Method:** A validated FE model of the L1-5 lumbar spine was used in this study. This FE model derived from computed tomography images of a healthy female adult volunteer of appropriate age. Then the model was modified to simulate L3-4 TLIF. Four conditions were compared: (i) intact; (ii) TLIF combined with bilateral pedicle screw fixation (BPSF); (iii) TLIF combined with U-shaped IPD Coflex-F (CF); and (iv) TLIF combined with unilateral pedicle screw fixation (UPSF). The intact and surgical FE models were analyzed under static and vibration loading conditions respectively. For static loading conditions, four motion modes (flexion, extension, lateral bending, and axial rotation) were simulated. For vibration loading conditions, the dynamic responses of lumbar spine under sinusoidal vertical load were simulated.

**Result:** Under static loading conditions, compared with intact case, BPSF decreased range of motion (ROM) by 92%, 95%, 89% and 92% in flexion, extension, lateral bending and axial rotation, respectively. While CF decreased ROM by 87%, 90%, 69% and 80%, and UPSF decreased ROM by 84%, 89%, 66% and 82%, respectively. Compared with CF, UPSF increased the endplate stress by 5%–8% in flexion, 7%–10% in extension, 2%–4% in lateral bending, and decreased the endplate stress by 16%–19% in axial rotation. Compared with CF, UPSF increased the cage stress by 9% in flexion, 10% in extension, and decreased the cage stress by 3% in lateral bending, and 13% in axial rotation. BPSF decreased the stress responses of endplates and cage compared with CF and UPSF. Compared BPSF, CF decreased the facet joint force (FJF) by 6%–13%, and UPSF decreased the FJF by 4%–12%. During vibration loading conditions, compared with BPSF, CF reduced maximum values of the FJF by 16%–32%, and vibration amplitudes by 22%–35%, while UPSF reduced maximum values by 20%–40%, and vibration amplitudes by 31%–45%.

**Conclusion:** Compared with other surgical models, BPSF increased the stability of lumbar spine, and also showed advantages in cage stress and endplate stress. CF showed advantages in IDP and FJF especially during vertical vibration, which may lead to lower risk of adjacent segment degeneration. CF may be an effective alternative to pedicle screw fixation in TLIF procedures.

**Key words:** Finite element; Interspinous process device; Pedicle screw fixation; Transforaminal lumbar interbody fusion; Whole body vibration

**Address for correspondence** Weiqiang Liu, PhD, Tsinghua Shenzhen International Graduate School, Tsinghua University, Shenzhen, China 518055. Tel: +86-0755-26551376; Fax: +86-0755-26551380; Email: [weiqiangliu19@163.com](mailto:weiqiangliu19@163.com)

Received 8 January 2021; accepted 2 July 2022

## Introduction

Transforaminal lumbar interbody fusion (TLIF) has been a common surgical procedure for the treatment of low back pain.<sup>1</sup> TLIF may cause less neurologic injury and allow a large footprint interbody cage through a small incision.<sup>2</sup> To achieve effective fusion, pedicle screw fixation is commonly used in conjunction with the TLIF procedure. Several studies have demonstrated the effectiveness of pedicle screw fixation in preventing subsidence and pseudoarthrosis.<sup>3,4</sup> However, previous studies have reported that the traditional pedicle screw system increased motion and stress at adjacent segments,<sup>5,6</sup> which may lead to adjacent segment degeneration (ASD) in the long term. According to previous clinical studies, the incidence of radiographic ASD ranged from 5.2% to 100%.<sup>7</sup> In addition, traditional pedicle screw fixation may be associated with complications such as screw misplacement, pedicle breakage, screw loosening, and loss of correction.<sup>8</sup> Biomechanical studies have also suggested that rigid pedicle screw system may lead to stress concentration in implants, especially in middle regions of the rods and neck regions of the screws.<sup>9</sup>

Recently, in order to reduce the undesirable complications of traditional lumbar fusion, the interspinous process device (IPD) has been developed as an alternative in treating lumbar degenerative diseases. An IPD is a flexible system which may preserve movement and improve load transmission of the lumbar spine.<sup>10</sup> By distraction of the distance between adjacent spinous processes, the diameter of the intervertebral foramen and spinal canal area is enlarged, and the dura and lumbar nerve roots are decompressed.<sup>11</sup> Compared with pedicle screw fixation, IPD may achieve comparable clinical and radiologic outcomes, with shorter operative time, less intraoperative blood loss, and shorter hospital stay.<sup>12</sup> Due to its minimal invasive characteristics, IPD has attracted more attention from surgeons and researchers in recent years. Some IPDs can be used stand-alone to maintain segmental motion,<sup>13,14</sup> such as X-Stop (Medtronic, Minneapolis, MN, USA), Coflex (Paradigm Spine, Wurmlingen, Germany), DIAM (Medtronic Sofamor Danek, Paris, France), and Wallis (Abbott Spine, Austin, TX, USA) systems, while the others can be used for supplementary fixation in lumbar interbody fusion,<sup>15</sup> such as Coflex-F (Paradigm Spine, Wurmlingen, Germany) and SPIRE (Medtronic, Memphis, TN, USA) systems.

Coflex-F is a U-shaped IPD which can be used as an adjunct to fusion. It is a modified structure of the original Coflex device (addition of two rivets) and can be more rigidly attached to spinous processes. Several studies have been conducted to investigate the biomechanical behavior of Coflex-F device. An *in vitro* study of Kettler *et al.*<sup>16</sup> showed that the Coflex-F device strongly stabilized the surgical segment especially in flexion, and decreased range of motion (ROM) in extension, lateral bending and axial rotation compared with other IPDs. Lo *et al.*<sup>17</sup> compared the biomechanics of Coflex-F combined with TLIF and anterior lumbar interbody fusion (ALIF) respectively. They found that

Coflex-F combined with TLIF had lower stability than when combined with ALIF. Guo *et al.*<sup>18</sup> also optimized the structure of Coflex-F device to decrease stress concentration in the implant. By topology optimization methods, they reduced the volume of Coflex-F device by 8%, and the optimized structure can provide stability at the surgical segment in all motion modes. Park *et al.*<sup>19</sup> studied the influence of the Coflex-F device on spinous process fracture by the finite element (FE) method. They reported that the addition of pre-tension on the Coflex-F device increased the stability at the surgical level in flexion and extension, but also increased spinous process fracture risk.

Although these studies have provided valuable insights into the biomechanics of the Coflex-F device, the influence of the Coflex-F device on cage subsidence and facet joint force (FJF) has not been investigated. Moreover, most previous studies were conducted under static loads, and the dynamic performance of the Coflex-F device under whole body vibration (WBV) remained unclear. In daily life, patients may be inevitably exposed to WBV caused by vehicles, which is more dangerous compared with static loads. In previous biomechanical research, Guo *et al.*<sup>20</sup> studied the stress responses of lumbar spine under vibration loads and static loads respectively. They reported that compared with static loads, vibration loads with equivalent magnitude (40 N) increased the axial displacement and intradiskal pressure (IDP) of lumbar spine by 314.5% and 242.4%. Therefore, it is necessary to study the dynamic performance of lumbar spine after surgery.

Using a validated FE model may be helpful in understanding the role of Coflex-F device in lumbar spine. Therefore, the aims of this FE study are: (i) to investigate the biomechanics of TLIF with Coflex-F and pedicle screw fixation; and (ii) to investigate the biomechanical effects of the Coflex-F device under both static and vibration conditions. One intact model (L1-5 lumbar spine) and three TLIF models with various fixation options were developed. Static and vibration loading conditions were performed respectively. The results of ROM, endplate stress, cage stress, FJF and IDP were calculated and analyzed.

## Materials and Methods

### Finite Element Models of the Lumbar Spine

A previously developed and validated FE model<sup>21</sup> of the intact human L1-5 lumbar spine was used in this study (Fig. 1A). The geometry of the lumbar spine was obtained from 0.7-mm-thick computed tomography (CT) scans of a healthy adult female without previous spinal degeneration or mental disease (age 37 years, height 158 cm, weight 52 kg). A total of 492 CT images were transformed into a 3D geometric model in medical format. Then the geometric model was meshed in Hypermesh (Altair Technologies, Inc., Fremont, CA, USA). This FE model included cortical bone, cancellous bone, posterior bone, intervertebral disk and seven kinds of ligaments. The thickness of cortical bone was

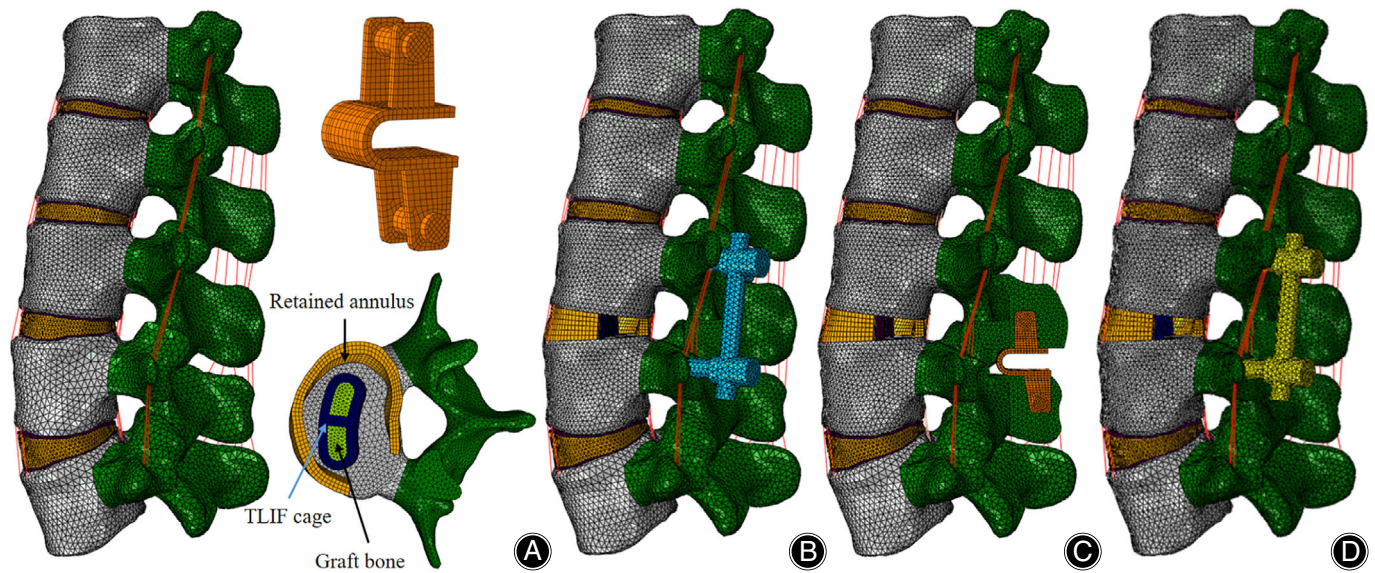


**Fig. 1** FE models of the lumbar spine. (A) Intact model; (B) TLIF with BPSF; (C) TLIF with CF; (D) TLIF with UPSF. The intact L1-5 lumbar model was established by scanning the lumbar of a 37-year-old female volunteer through 0.7-mm-thick CT. The geometric model was meshed in Hypermesh software

1 mm, and the thickness of cartilaginous endplate was 0.5 mm. All the ligaments were meshed by tension-only truss elements. The contact between the facet joints was simulated by frictionless surface-to-surface contact.<sup>22-24</sup> The intact model included 120,978 nodes and 555,063 elements. Finally, the L1-5 lumbar spine model was imported into Abaqus (Simulia, Inc., Providence, RI, USA) to perform FE analysis. The computer for the simulation is Think Station (Lenovo Group Ltd, Beijing, China.) with 64 GB memory and 24 processors.

Two loading conditions were implemented. The first loading condition was for validation of the intact FE model. With the inferior surface of L5 fixed in all directions, four pure moments (8 Nm flexion, 6 Nm extension, 6 Nm lateral bending, and 4 Nm torsion) were applied at the center of the superior surface of L1. Furthermore, by applying increasing preload values to the lumbar model (100, 200, 300, and 400 N), the IDP and the axial displacement of L4-5 were compared with the previous experimental results. The second loading condition was applied to both intact and surgical models to evaluate biomechanical behaviors. A moment of 7.5 Nm was applied at the center of the superior surface of L1 to simulate flexion, extension, lateral bending, and torsion motion. In addition, a 280 N follower load, which represents the partial body weight, 12 was applied along the curvature of the lumbar spine bilaterally using a set of connector elements. For surgical models, the displacement control was applied to obtain the same L1-5 ROM of the intact model. Finally, the ROM, IDP, and FJF were calculated.

To simulate the TLIF procedure, total nucleus pulposus, partial annulus and unilateral facet joint were

removed at the L3-4 segment. The TLIF cage was inserted at the L3-4 disk space with various fixation options (Figs 1B,C, D). The following conditions were compared: (i) intact; (ii) TLIF combined with bilateral pedicle screw fixation (BPSF); (iii) TLIF combined with Coflex-F (CF); and (iv) TLIF combined with unilateral pedicle screw fixation (UPSF). The pedicle screws (45 mm in length and 6 mm in diameter) were interconnected by longitudinal rods (6 mm in diameter). In order to simulate the long-term effects after instrumentation, the bone-screw and bone-cage interfaces were set as tie constraints.<sup>25,26</sup> For the Coflex-F device (8 mm in height), the teeth were simplified by assigning a high friction coefficient of 0.8, and the friction coefficient was set to 0.1 for the rest of the contact areas.<sup>19</sup> The material properties were summarized in Table 1.

#### Model Validation

The intact L1-5 FE model was validated against the previous experimental results. With four pure moments applied at the L1 segment, the predicted ROMs were compared with the results of a previously published cadaveric study by Renner *et al.*<sup>27</sup> In addition, by applying increasing preload values to the lumbar spine, the IDP and axial displacement of L4-5 were compared with the experimental results by Berkson *et al.*<sup>28</sup> and Brinckmann *et al.*<sup>29</sup>

#### Boundary Conditions

The inferior surface of the L5 segment was constrained in all directions. A follower load of 280 N was applied along the curvature of the lumbar spine bilaterally to represent the physiologic compressive loading induced by muscles.



**TABLE 1** Material properties used in the FE models

Component	Young's modulus (MPa)	Poisson ratio	Cross-sectional area (mm <sup>2</sup> )	Density (kg/mm <sup>3</sup> )
Cortical bone	12,000	0.3		1.7e-6
Cancellous bone	100	0.2		1.1e-6
Posterior bone	3500	0.25		1.4e-6
Endplate	24	0.25		1.2e-6
Nucleus pulposus	1	0.49		1.02e-6
Annulus fibrosus	4.2	0.45		1.05e-6
Anterior longitudinal	20	0.3	63.7	1.0e-6
Posterior longitudinal	20	0.3	20	1.0e-6
Ligament flava	19.5	0.3	40	1.0e-6
Interspinal	11.6	0.3	40	1.0e-6
Supraspinal	15	0.3	30	1.0e-6
Intertransverse	58.7	0.3	3.6	1.0e-6
Capsular	32.9	0.3	60	1.0e-6
Pedicle screws (Ti)	110,000	0.3		4.5e-6
Coflex-F (Ti)	110,000	0.3		4.5e-6
Cage	3500	0.3		1.32e-6

The static and vibration loading conditions were performed respectively. For static loading conditions, a moment of 7.5 Nm was applied to the L1 segment of the intact model to simulate four motion modes (flexion, extension, lateral

bending and axial rotation). The hybrid loading method was applied to the surgical models to produce the same amount of motion of the intact model in four motion modes. For vibration conditions, a sinusoidal vertical load of ±40 N,

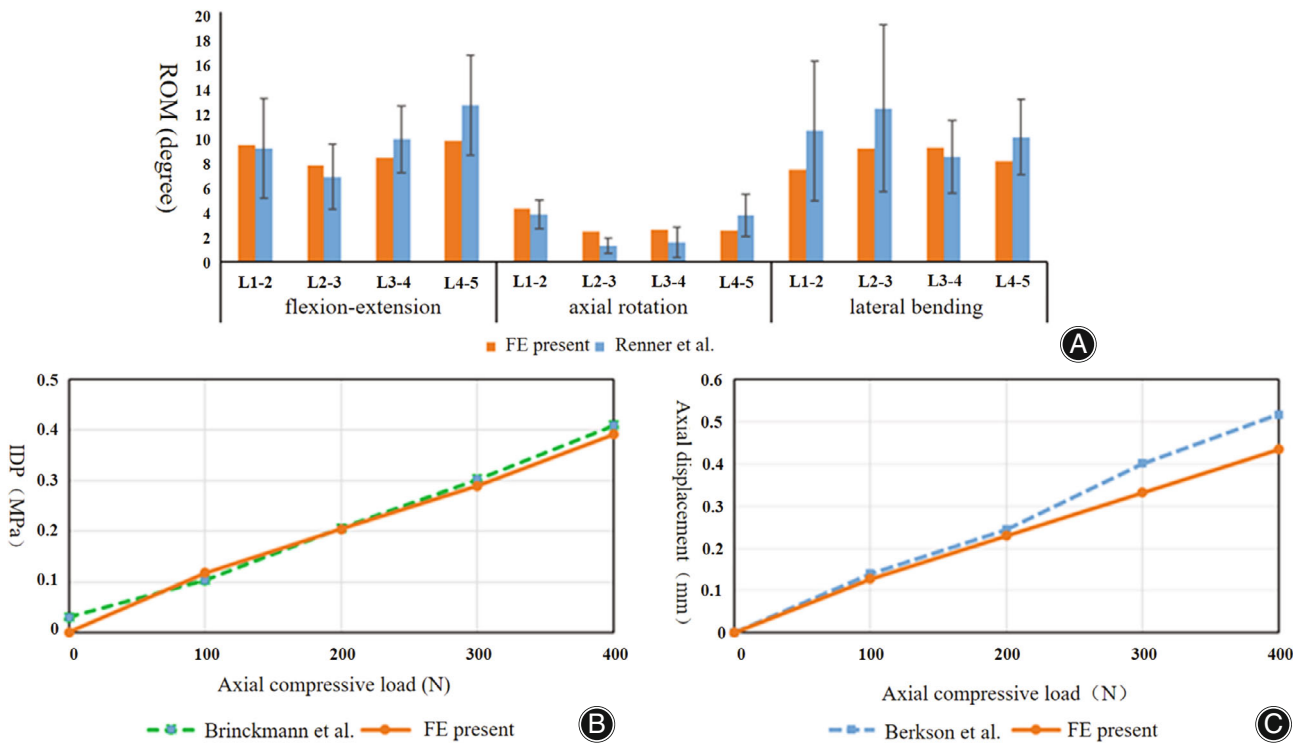


**Fig. 2** Comparison between the current FE model and previous *in vitro* study. (A) ROM of each segment; (B) L4-5 IDP; (C) L4-5 axial displacement. According to the figure, the predicted results of the current FE model were comparable to the results of *in vitro* studies

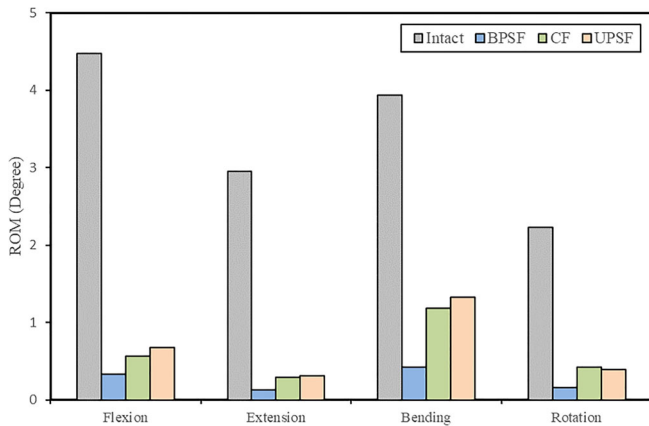


**Fig. 3** ROM at the fusion segment in four motion modes. According to the figure, BPSF provided the highest stability at the surgical segment. Compared with UPSF, the ROM of CF was lower in flexion, extension and lateral bending, but higher in axial rotation

which simulated the WBV conditions of human body, was imposed on the superior surface of the L1 segment at a frequency of 5 Hz, and the loading duration was 2 s.<sup>30</sup>

**Main Outcomes**

The following parameters were investigated in this study.

*Range of Motion*

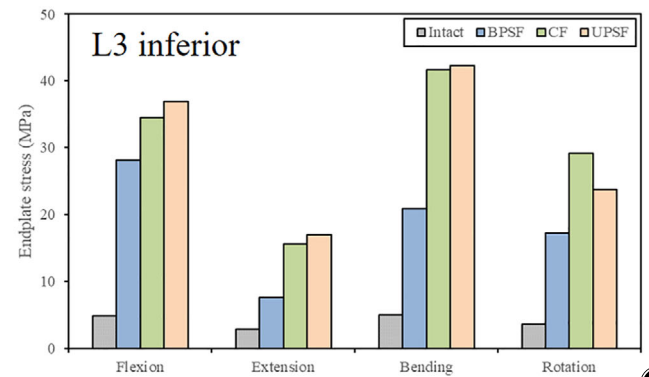
Range of motion was defined as the rotation angle of each segment of the lumbar spine. In this study, the inferior surface of the L5 segment was fixed in all directions, and the rotation angle of each segment was measured. For example, the range of motion of L3-4 segment was equal to the rotation angle of L3 minus the rotation angle of L4. Range of motion was one of the most important indicators to assess the lumbar motion function.

*Endplate Stress*

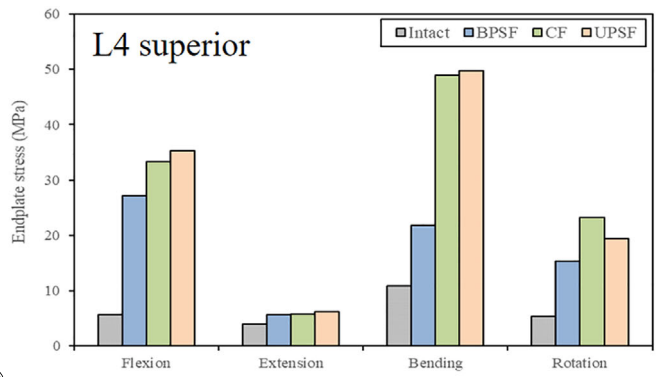
Endplate stress was defined as the maximum value of the stresses in the elements used to model the cartilage endplate. This parameter represented the loads transmitted to the adjacent segments, and was one of the most important indicators to assess the risk of cage subsidence.

*Cage Stress*

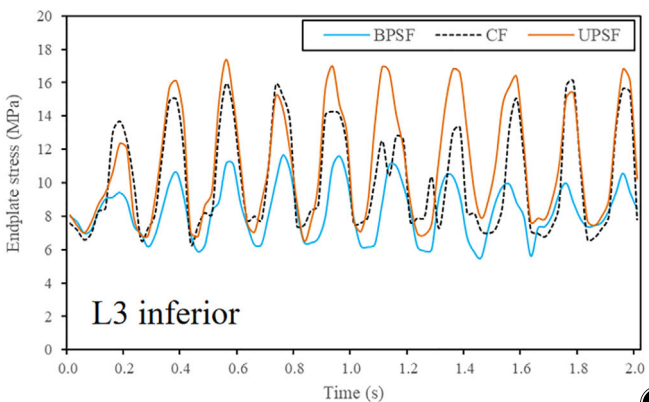
Cage stress was defined as the maximum value of the stresses in the elements used to model the cage. This parameter



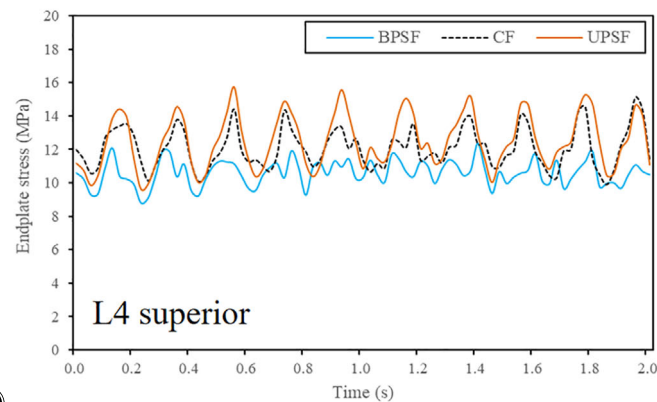
(A)



(B)



(C)



(D)

**Fig. 4** Endplate stress. (A) Maximum stress of the L3 inferior endplate under static loads; (B) Maximum stress of the L4 superior endplate under static loads; (C) Dynamic responses of the L3 inferior endplate stress; (D) Dynamic responses of the L4 superior endplate stress. According to the figure, compared among the surgical models, BPSF produced the lowest endplate stresses during both static and vibration loading conditions

represented the effective loads on the cage, and was investigated to assess the risk of implant breakage and cage subsidence.

#### Facet Joint Force

Facet joint force was defined as the average value of the contact force in the elements used to model the facet joints. This parameter represented the bearing capacity of the facet joint, and was one of the indicators to assess facet joint pain.

#### Intradiscal Pressure

Intradiscal pressure was defined as the maximum value of the pressures in the elements used to model the intervertebral disk. This parameter represented the pressure transmitted by the intervertebral disk, and was one of the most indicators to assess the risk of lumbar degeneration.

## Results

#### Model Validation

Under four pure moments, the ROM of each segment was validated. The predicted ROM was within one standard deviation of the results derived from the biomechanical cadaver measurements (Fig. 2A). Under increasing preload values, the predicted results of the L4-5 IDP and axial displacement were also comparable to the results of previous *in vitro* studies (Figs 2B,C). Therefore, the FE model was proved to be valid and reliable.

**TABLE 2** Quantitative comparisons of biomechanical performance during static loading conditions

Range of motion	UPSF	≥	CF	>	BPSF
Endplate stress	UPSF	≈	CF	>	BPSF
Cage stress	UPSF	≈	CF	>	BPSF
Facet joint force	BPSF	>	CF	≈	UPSF
Intradiscal pressure	BPSF	>	UPSF	≈	CF

#### Range of Motion

Under static loading conditions, the predicted ROM at surgical segment was displayed in Fig. 3. After the TLIF procedure, the ROM decreased substantially in all motion modes. Compared with intact case, ROM of BPSF decreased by 92%, 95%, 89% and 92% in flexion, extension, lateral bending and axial rotation, respectively. In addition, ROM of CF decreased by 87%, 90%, 69% and 80%, and ROM of UPSF decreased by 84%, 89%, 66% and 82%. Compared among surgical models, ROM of BPSF was the minimum in all motion modes. Compared with UPSF, CF showed lower ROM in flexion, extension and lateral bending.

#### Endplate Stress

Figures 4A,B compared the maximum endplate stresses under static loads. After TLIF surgery, the predicted endplate stresses increased significantly in all motion modes. Compared with other surgical models, BPSF demonstrated the lowest endplate stress. Compared with CF, UPSF increased the endplate stress by 5%–8% in flexion, 7%–10% in extension, and 2%–4% in lateral bending, respectively. While in axial rotation, UPSF decreased the endplate stress by 16%–19% compared with CF.

Under vertical vibration, the dynamic responses of endplate stresses were displayed in Figs 4C,D. The results of the maximum and minimum values and vibration amplitudes are summarized in Table 2. Compared with other surgical models, BPSF demonstrated the lowest dynamic responses of the endplate stresses, followed by CF. Compared with BPSF, CF increased maximum values of the endplate stresses by 22%–38%, and vibration amplitudes by 46%–59%, while UPSF increased maximum values by 26%–49%, and vibration amplitudes by 70%–77%.

#### Cage Stress

Under static loading conditions, the cage stress was displayed in Fig. 5A. Cage stress of BPSF was lower than those of CF

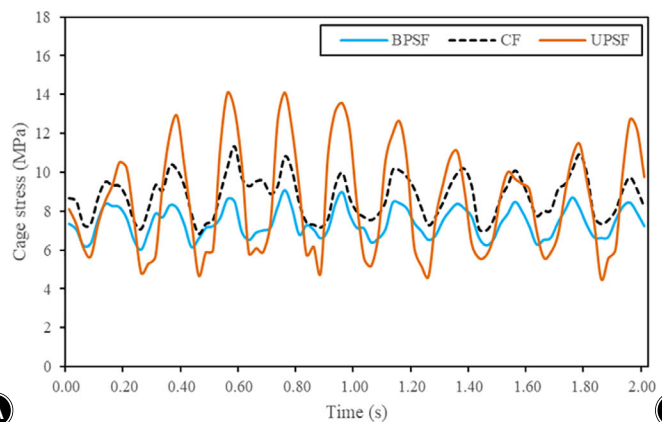
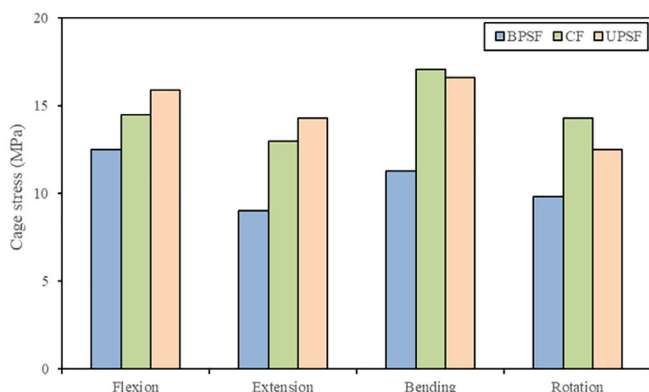


**Fig. 5** Cage stress. (A) Maximum cage stress under static loads; (B) Dynamic responses of the cage stress. According to the figure, compared among the surgical models, BPSF showed the lowest cage stresses during both static and vibration loading conditions

and UPSF in all motion modes. Compared with CF, UPSF increased the cage stress by 9% in flexion, 10% in extension, and decreased the cage stress by 3% in lateral bending, and 13% in axial rotation, respectively.

Under vertical vibration, the dynamic responses of cage stress are shown in Fig. 5B. UPSF showed significantly higher dynamic responses of cage stress than those of BPSF and CF. Compared with UPSF, BPSF reduced maximum values of the cage stress by 35%, and vibration amplitudes by 68%, while CF reduced maximum values by 20%, and vibration amplitudes by 53%, respectively.

### Facet Joint Force

Figures 6A,B displayed the FJF at adjacent segments under static loads. FJF of BPSF was slightly higher than those of CF and UPSF in all motion modes except for flexion. Compared with BPSF, CF decreased the FJF by 6%–7% in extension, 6%–13% in lateral bending, and 7%–11% in axial rotation, while UPSF decreased the FJF by 9%–11% in extension, 8%–12% in lateral bending, and 4%–6% in axial rotation, respectively.

Under WBV, the dynamic responses of FJF were shown in Figs 6C,D. It was observed that CF and UPSF showed similar FJF during vertical vibration, while BPSF demonstrated the highest dynamic responses. Compared with BPSF, CF reduced maximum values of the FJF by 16%–32%, and vibration amplitudes by 22%–35%, while UPSF reduced maximum values by 20%–40%, and vibration amplitudes by 31%–45%.

### Intradiskal Pressure

Under static loads, the IDPs at adjacent levels were displayed in Figs 7A,B. After TLIF, the IDPs at adjacent levels increased in all motion modes. The IDP of BPSF was slightly higher than those of CF and UPSF. Compared among all surgical models, CF showed the lowest IDP in axial rotation.

Under vertical vibration, the dynamic responses of IDPs at adjacent levels were shown in Figs 7C,D. UPSF demonstrated the highest dynamic responses of IDP, followed by BPSF. Compared with UPSF, BPSF decreased maximum values of the IDP by 8%–11%, and vibration amplitudes by 9%–16%, while CF decreased maximum values by 31%–33%, and vibration amplitudes by 36%–46%, respectively.<sup>30</sup>

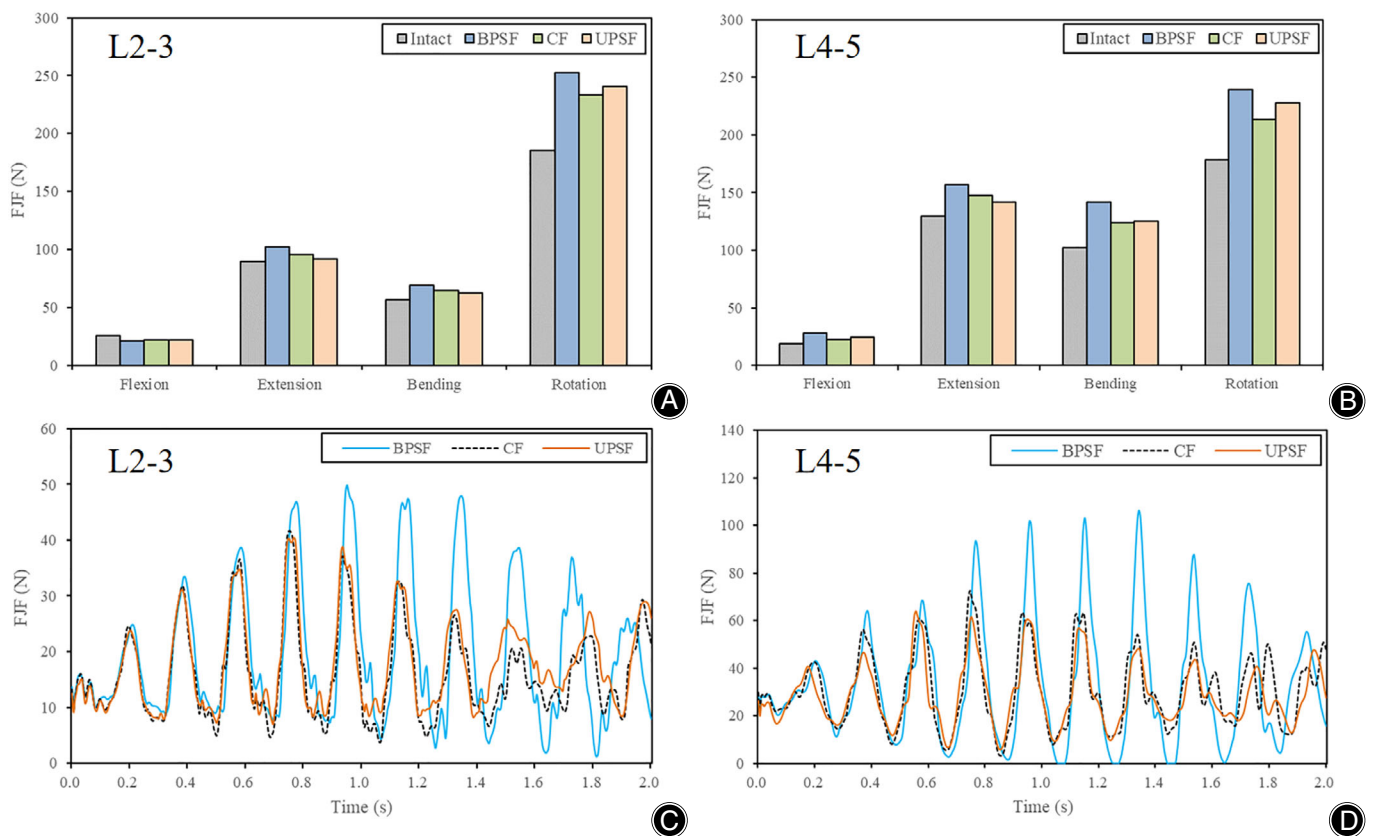


**Fig. 6** FJF at adjacent levels. (A) L2-3 FJF under static loads; (B) L4-5 FJF under static loads; (C) Dynamic responses of L2-3 FJF under vertical vibration; (D) Dynamic responses of L4-5 FJF under vertical vibration. According to the figure, compared with BPSF, CF and UPSF showed advantages in FJF at adjacent segments during both static and vibration loading conditions

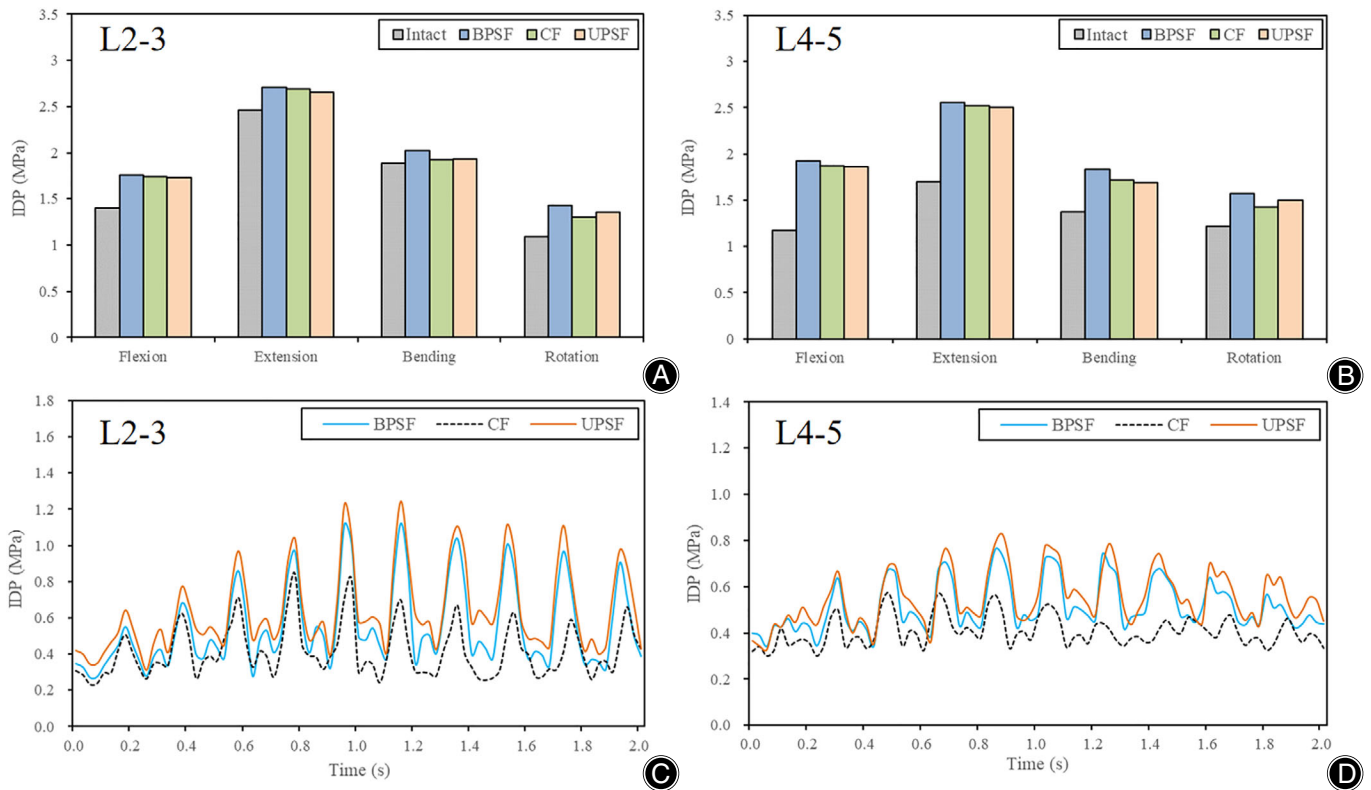


**Fig. 7** IDP at adjacent segments. (A) L2-3 IDP under static loads; (B) L4-5 IDP under static loads; (C) Dynamic responses of the L2-3 IDP; (D) Dynamic responses of the L4-5 IDP. According to the figure, compared among the surgical models, *CF* showed the lowest IDP especially during vibration loading conditions

## Discussion

### Influence of Static Loading Conditions on Biomechanics

The aim of IPD is to enhance the stability after alleviating the nerve compression at the surgical segment.<sup>31</sup> Previous clinical literatures reported that stand-alone IPDs achieved satisfactory results in the short-to-long term.<sup>32</sup> In the current study, static analysis was performed on the FE models under flexion, extension, lateral bending and axial rotation. Although the unilateral pedicle screw fixation for TLIF has been proved with satisfactory clinical outcomes,<sup>33</sup> several biomechanical studies demonstrated that it is significantly less stable than BPSF.<sup>34</sup> In current research, as shown in Fig. 3, a similar trend was found. In addition, compared with UPSF, the ROM of *CF* was lower in flexion, extension and lateral bending, but higher in axial rotation. One possible reason may be that the Coflex-F device distracted the facet joints, which are essential in controlling axial rotation.<sup>11</sup> The risk of cage subsidence may be associated with the stresses in cage and endplates.<sup>35</sup> Compared with UPSF, as shown in Figs 4A,B and 5A, BPSF produced significantly lower endplate stress and cage stress in four motion modes, implying a lower risk of subsidence in BPSF model. Fang *et al.*<sup>36</sup> also reported that BPSF could reduce the maximum stresses

on the endplate, especially in flexion and extension, which was consistent with the findings of the current study.

In addition, *CF* decreased the stresses in cage and endplates in flexion and extension compared with UPSF. At adjacent segments, *CF* and UPSF showed smaller values of IDP and FJF than BPSF in four motion modes (Figs 6A,B and 7A,B), which may be beneficial to prevent adjacent segment degeneration in the long term. This finding was consistent with the results of Guo *et al.*<sup>5</sup> who reported that stiffer posterior fixation increased the load at adjacent segments. Table 2 quantitatively compared the biomechanical performance of *CF*, BPSF and UPSF during static loading conditions. In general, under static loading conditions, the influence of *CF* was between that of BPSF and UPSF.

### Effects of Vibration Loading Conditions on Biomechanics

Previous studies have reported that vertical vibration significantly increased stresses in lumbar disks,<sup>20</sup> which is more dangerous compared with static loading conditions.<sup>9,20</sup> However, few studies have investigated the dynamic performance of TLIF with Coflex-F and pedicle screw fixation during WBV. Therefore, in the current study, an axial sinusoidal load of  $\pm 40\text{N}$  at a frequency of 5 Hz was applied for vertical



vibration condition. This load mode was also adopted in previous studies to simulate the condition when a person was sitting in vehicles,<sup>3,9</sup> and the value of 5Hz was close to the experimental results of the first resonant frequency of human lumbar spine.<sup>37</sup> As displayed in Figs 4C,D and 5B, during vertical vibration, BPSF showed the lowest stress responses in endplates and cage. This result implied that BPSF may have a lower risk of cage subsidence during vertical vibration, which agreed with a previous FE study.<sup>3</sup> BPSF decreased the vibration amplitudes of endplate stresses by 46.4%–48.0%. In addition, the current study also found that CF decreased the stress responses in endplates and cage compared with UPSF. At adjacent segments, CF and UPSF significantly decreased the dynamic responses of FJF compared with BPSF (Figs 6C,D). Furthermore, CF also showed the lowest dynamic responses in IDP compared among all the surgical models (Figs 7C,D). This may be explained by the flexibility of the Coflex-F device, and its U-shaped structure absorbed some vibration energy during WBV. This finding implies that CF may be beneficial to alleviate adjacent segment disease and facet joint pain, especially during vertical vibration. Table 3 quantitatively compared the biomechanical performance of CF, BPSF and UPSF during vibration loading conditions. Table 4 summarized the results of the dynamic responses.

### Main Findings Analysis of this Study

Previous studies have evaluated the biomechanical effects of IPD under static loads. Some biomechanical studies<sup>16,18</sup>

reported that IPD mainly controlled ROM in flexion and extension, but with less influence on lateral bending and rotation. This finding was consistent with the results of the current study (Fig. 3). One previous FE study<sup>17</sup> also reported that IPD resulted in higher endplate stresses and lower ROMs than pedicle screw fixation at surgical segment, and a similar trend was found in current research (Fig. 4). In addition, we found that IPD decreased the stresses at adjacent segments compared with bilateral pedicle screws, which was consistent with the findings of Guo *et al.*<sup>5</sup> who reported that BPSF increased the IDP by 99%–116%, and FJF by 18%–60% at adjacent segments. In addition to static loads, we also simulated vibration loading conditions.

Our results showed that BPSF increased the stability of the lumbar spine, and it also decreased the stress responses of endplates and cage under both static and vibration conditions, which may be associated with a lower risk of cage subsidence. However, BPSF produced higher stress responses at adjacent segments, implying a higher risk of adjacent segment degeneration. In a previous FE study conducted by Wang *et al.*,<sup>38</sup> the results showed that BPSF significantly increased the ROM at adjacent segments by 5%–51%, which was much higher than that in IPD fixation. Compared with BPSF, UPSF decreased the stresses at adjacent segments, but some studies have reported that UPSF was not stable enough to prevent cage migration.<sup>33</sup> One possible reason may be that UPSF resulted in asymmetry.<sup>33</sup> In general, under static loading condition, the influence of CF was between that of UPSF and BPSF. During vertical vibration, CF significantly decreased the stress responses of IDP and FJF at adjacent segments. Therefore, from a biomechanical point of view, CF may offer an alternative to traditional pedicle screw fixation in TLIF procedures. Certainly, it should be pointed out that there were associated complications of using IPDs for lumbar diseases, such as spinous process fracture and device dislocation.<sup>39,40</sup> The higher reoperation rate was also an important factor. The usage of IPD should be evaluated discreetly.

**TABLE 3** Quantitative comparisons of biomechanical performance during vibration loading conditions

Endplate stress	UPSF	>	CF	>	BPSF
Cage stress	UPSF	>	CF	>	BPSF
Facet joint force	BPSF	>	UPSF	≈	CF
Intradiscal pressure	UPSF	>	BPSF	>	CF

**TABLE 4** The maximum and minimum values and vibration amplitudes of the dynamic responses

Dynamic responses	BPSF			CF	UPSF				
	Max	Min	VA		Max	Min	VA		
Endplate stress (MPa)									
L3 inferior	11.66	5.52	6.14	16.09	6.35	9.74	17.36	6.54	10.82
L4 superior	12.39	8.81	3.58	15.15	9.90	5.25	15.73	9.63	6.10
Cage stress (MPa)									
TLIF cage	9.10	6.02	3.08	11.34	6.86	4.48	14.09	4.49	9.60
FJF (N)									
L2-3	49.89	1.26	48.63	41.59	3.78	37.81	40.36	7.09	33.27
L4-5	106.24	0	106.24	72.44	3.12	69.32	64.06	5.63	58.43
IDP (MPa)									
L2-3	1.12	0.27	0.85	0.84	0.24	0.60	1.25	0.31	0.94
L4-5	0.76	0.34	0.42	0.57	0.30	0.27	0.83	0.33	0.50

Abbreviations: Max, maximum value; Min, minimum value; VA, vibration amplitude, VA = Max – Min.

### Limitations

The limitations in the present FE study should be pointed out. First, only one unique FE model was employed, the simulated results might not be representative of average person. In the current model, the material properties were simplified to be linear elastic although the components of lumbar spine have nonlinear material property in reality. However, the tendency of the predicted results would not be significantly changed. In addition, although a follower load was applied, it could not thoroughly represent the passive effects of the muscles, which played an important role in lumbar spine stabilization. Furthermore, the current FE model did not simulate degenerative characteristics such as collapsed disk height, spondylolisthesis, or degenerative facet joints.

### Conclusion

The current study investigated the biomechanical performance of TLIF with Coflex-F or pedicle screw fixation under both static and vibration loading conditions. Compared with other surgical models, BPSF increased the stability of lumbar spine, and also showed advantages in cage stress and endplate stress. Under static loading conditions, the influence

of CF was between that of UPSF and BPSF. During vertical vibration, CF showed advantages in IDP and FJF, which may lead to lower risk of adjacent segment degeneration. From a biomechanical point of view, CF may be an effective alternative to pedicle screw fixation in TLIF procedures. In clinical practice, the usage of IPD should be evaluated discreetly.

### Author Contribution

Jia Zhu and Hangkai Shen drafted the manuscript, revised this article and wrote this article completely. Jia Zhu and Yangyang Cui assisted with literature search of the FE model. Guy R. Fogel provided research ideas and guided article writing. Professor Weiqiang Liu and Zhenhua Liao supervised this study.

### Funding Information

This study was supported by the China National Key Research and Development Plan Project (2016YFC1102002) and the Application Demonstration Project of Shenzhen (KJYY20170405161248988).

### References

- Sivaganesan A, Hirsch B, Phillips FM, McGirt MJ. Spine surgery in the ambulatory surgery center setting: value-based advancement or safety liability? *Neurosurgery*. 2018;83:159–65.
- Faizan A, Kiapour A, Kiapour AM, Goel VK. Biomechanical analysis of various footprints of transforaminal lumbar interbody fusion devices. *J Spinal Disord Tech*. 2014;27:118–27.
- Fan W, Guo LX. The role of posterior screw fixation in single-level transforaminal lumbar interbody fusion during whole body vibration: a finite element study. *World Neurosurg*. 2018;114:1086–93.
- Xiao SW, Jiang H, Yang LJ, Xiao ZM. Comparison of unilateral versus bilateral pedicle screw fixation with cage fusion in degenerative lumbar diseases: a meta-analysis. *Eur Spine J*. 2015;24:764–74.
- Guo LX, Wang QD. Biomechanical analysis of a new bilateral pedicle screw fixator system based on topological optimization. *Int J Precis Eng Manuf*. 2020;21:1363–74.
- Guo TM, Lu J, Xing YL, Liu GX, Zhu HY, Yang L, et al. A 3-dimensional finite element analysis of adjacent segment disk degeneration induced by transforaminal lumbar interbody fusion after pedicle screw fixation. *World Neurosurg*. 2019;124:51–7.
- Park P, Garton HJ, Gala VC, Hoff JT, McGillicuddy JE. Adjacent segment disease after lumbar or lumbosacral fusion: review of the literature. *Spine (Phila Pa 1976)*. 2004;29:1938–44.
- Choi J, Kim S, Shin D-A. Biomechanical comparison of spinal fusion methods using interspinous process compressor and pedicle screw fixation system based on finite element method. *J Korean Neurosurg Soc*. 2016;59:91–7.
- Fan W, Guo LX, Zhao D. Stress analysis of the implants in transforaminal lumbar interbody fusion under static and vibration loadings: a comparison between pedicle screw fixation system with rigid and flexible rods. *J Mater Sci Mater Med*. 2019;30:118.
- Kabir SMR, Gupta SR, Casey ATH. Lumbar interspinous spacers a systematic review of clinical and biomechanical evidence. *Spine (Phila Pa 1976)*. 2010;35:1499–506.
- Chen CS, Shih SL. Biomechanical analysis of a new lumbar interspinous device with optimized topology. *Med Biol Eng Comput*. 2018;56:1333–41.
- Li M, Yang HL, Wang GL. Interspinous process devices for the treatment of neurogenic intermittent claudication: a systematic review of randomized controlled trials. *Neurosurg Rev*. 2017;40:529–36.
- Du MR, Wei FL, Zhu KL, Song RM, Huan Y, Jia B, et al. Coflex interspinous process dynamic stabilization for lumbar spinal stenosis: long-term follow-up. *J Clin Neurosci*. 2020;81:462–8.
- Meyer B, Baranto A, Schils F, Collignon F, Zoega B, Tan L, et al. Percutaneous interspinous spacer vs decompression in patients with neurogenic claudication: an alternative in selected patients? *Neurosurgery*. 2018;82:621–9.
- Techy F, Mageswaran P, Colbrunn RW, Bonner TF, McLain RF. Properties of an interspinous fixation device (ISD) in lumbar fusion constructs: a biomechanical study. *Spine J*. 2013;13:572–9.
- Kettler A, Drumm J, Heuer F, Haeussler K, Mack C, Claes L, et al. Can a modified interspinous spacer prevent instability in axial rotation and lateral bending? A biomechanical in vitro study resulting in a new idea. *Clin Biomech (Bristol, Avon)*. 2008;23:242–7.
- Lo CC, Tsai KJ, Zhong ZC, Chen SH, Hung CH. Biomechanical differences of Coflex-F and pedicle screw fixation combined with TLIF or ALIF—a finite element study. *Comput Methods Biomech Biomed Engin*. 2011;14:947–56.
- Guo LX, Yin JY. Finite element analysis and design of an interspinous device using topology optimization. *Med Biol Eng Comput*. 2019;57:89–98.
- Park WM, Choi DK, Kim YH, Kim K. Pre-tension effects from tightening the ligature on spinous process fracture risk in interspinous process device implantation. *Int J Precis Eng Manuf*. 2014;15:2597–604.
- Guo LX, Fan W. Dynamic response of the lumbar spine to whole-body vibration under a compressive follower preload. *Spine (Phila Pa 1976)*. 2018;43:143–53.
- Shen HK, Fogel GR, Zhu J, Liao ZH, Liu WQ. Biomechanical analysis of different lumbar interspinous process devices: a finite element study. *World Neurosurg*. 2019;127:1112–9.
- Choi J, Shin DA, Kim S. Biomechanical effects of the geometry of ball-and-socket artificial disc on lumbar spine. *Spine (Phila Pa 1976)*. 2017;42:332–9.
- Wang BJ, Ke WC, Hua WB, Lu SD, Zeng XL, Yang C. Biomechanical evaluation of anterior and posterior lumbar surgical approaches on the adjacent segment: a finite element analysis. *Comput Methods Biomech Biomed Engin*. 2020;23:1109–16.
- Choi J, Shin DA, Kim S. Finite element analysis of a ball-and-socket artificial disc design to suppress excessive loading on facet joints: a comparative study with ProDisc. *Int J Numer Method Biomed Eng*. 2019;35:1–9.
- Fan W, Guo LX. A comparison of the influence of three different lumbar interbody fusion approaches on stress in the pedicle screw fixation system: finite element static and vibration analyses. *Int J Numer Method Biomed Eng*. 2019;35:e3162. <https://doi.org/10.1002/cnm.3162>
- Li J, Wang WK, Zuo R, Zhou Y. Biomechanical stability before and after graft fusion with unilateral and bilateral pedicle screw fixation: finite element study. *World Neurosurg*. 2019;123:228–34.
- Renner SM, Natarajan RN, Patwardhan AG, Havey RM, Voronov LI, Guo BY, et al. Novel model to analyze the effect of a large compressive follower preload on range of motions in a lumbar spine. *J Biomech*. 2007;40:1326–32.
- Berkson MH, Nachemson A, Schultz AB. Mechanical-properties of human lumbar spine motion segments. 2. responses in compression and shear— influence of gross morphology. *J Biomech Eng*. 1979;101:53–7.
- Brinckmann P, Grootenboer H. Change of disk height, radial disk bulge, and intradiscal pressure from discectomy—an invitro investigation on human lumbar disks. *Spine (Phila Pa 1976)*. 1991;16:641–6.
- Guo LX, Fan W. Impact of material properties of intervertebral disc on dynamic response of the human lumbar spine to vertical vibration: a finite element sensitivity study. *Med Biol Eng Comput*. 2019;57:221–9.

- 31.** Gu HL, Chang YB, Zeng SX, Zheng XQ, Zhang RY, Zhan SQ, et al. Wallis interspinous spacer for treatment of primary lumbar disc herniation: three-year results of a randomized controlled trial. *World Neurosurg.* 2018;120:1331–6.
- 32.** Mo ZM, Li D, Zhang RW, Chang MM, Yang BB, Tang SJ. Comparative effectiveness and safety of posterior lumbar interbody fusion, Coflex, Wallis, and X-stop for lumbar degenerative diseases: a systematic review and network meta-analysis. *Clin Neurol Neurosurg.* 2018;172:74–81.
- 33.** Lu P, Pan T, Dai T, Chen G, Shi KQ. Is unilateral pedicle screw fixation superior than bilateral pedicle screw fixation for lumbar degenerative diseases: a meta-analysis. *J Orthop Surg Res.* 2018;13:296–308.
- 34.** Ambati DV, Wright EK, Lehman RA, Kang DG, Wagner SC, Dmitriev AE. Bilateral pedicle screw fixation provides superior biomechanical stability in transforaminal lumbar interbody fusion: a finite element study. *Spine J.* 2015;15:1812–22.
- 35.** Zhang ZJ, Li H, Fogel GR, Xiang DD, Liao ZH, Liu WQ. Finite element model predicts the biomechanical performance of transforaminal lumbar interbody fusion with various porous additive manufactured cages. *Comput Biol Med.* 2018; 95:167–74.
- 36.** Fang GF, Lin YZ, Wu JC, Cui WG, Zhang SH, Guo LL, et al. Biomechanical comparison of stand-alone and bilateral pedicle screw fixation for oblique lumbar interbody fusion surgery—a finite element analysis. *World Neurosurg.* 2020;141: 204–12.
- 37.** Wilder DG, Woodworth BB, Frymoyer JW, Pope MH. Vibration and the human spine. *Spine (Phila Pa 1976).* 1982;7:243–54.
- 38.** Wang BJ, Hua WB, Ke WC, Lu SD, Li XS, Zeng XL, et al. Biomechanical evaluation of transforaminal lumbar interbody fusion and oblique lumbar interbody fusion on the adjacent segment: a finite element analysis. *World Neurosurg.* 2019;126:819–24.
- 39.** Poetscher AW, Gentil AF, Ferretti M, Lenza M. Interspinous process devices for treatment of degenerative lumbar spine stenosis: a systematic review and meta-analysis. *PLoS One.* 2018;13:e0199623. <https://doi.org/10.1371/journal.pone.0199623>
- 40.** Zhao X-w, Ma J-x, Ma X-l, Li F, He W-w, Jiang X, et al. Interspinous process devices(IPD) alone versus decompression surgery for lumbar spinal stenosis(LSS): a systematic review and meta-analysis of randomized controlled trials. *Int J Surg.* 2017;39:57–64.